Kinetic Analysis of Single Sodium Channels from Canine Cardiac Purkinje Cells

B. E. SCANLEY, D. A. HANCK, T. CHAY, and H. A. FOZZARD

From the Cardiac Electrophysiology Laboratories, Departments of Medicine and Pharmacological and Physiological Sciences, University of Chicago, Chicago, Illinois 60637; and the Department of Biological Sciences, University of Pittsburgh, Pittsburgh, Pennsylvania 15260

ABSTRACT Single sodium channel events were recorded from cell-attached patches on single canine cardiac Purkinje cells at 10–13°C. Data from four patches containing two to four channels and one patch with one channel were selected for quantitative analysis. The channels showed prominent reopening behavior at voltages near threshold, and the number of reopenings declined steeply with depolarization. Mean channel open time was a biphasic function of voltage with the maximum value (1–1.5 ms) occurring between −50 and −40 mV and lower values at more and at less hyperpolarized levels. Inactivation without opening was also prominent near threshold, and this occurrence also declined with depolarization. The waiting time distributions and the probability of being open showed voltage and time dependence as expected from whole-cell current studies. The results were analyzed in terms of a five-state Markovian kinetic model using both histogram analysis and a maximum likelihood method to estimate kinetic parameters. The kinetic parameters of the model fits were similar to those of GH_3 pituitary cells (Horn, R., and C. A. Vandenberg. 1984. *Journal of General Physiology.* 84:505–534) and N1E115 neuroblastoma cells (Aldrich, R. W., and C. F. Stevens. *Journal of Neuroscience.* 7:418–431). Both histogram and maximum likelihood analysis implied that much of the voltage dependence of cardiac Na current is in its activation behavior, with inactivation showing modest voltage dependence.

INTRODUCTION

The recent development of the patch-clamp technique for recording current through single Na channels (Sigworth and Neher, 1980) has permitted a reevaluation of the kinetic properties of the Na current. Individual channels open stochastically for relatively short intervals, so that Na current "activation" in the conventional Hodgkin-Huxley sense represents mobilization of channel openings, and Na current "inactivation" represents declining numbers of channel openings that occur after the peak of the macroscopic current (Aldrich et al., 1983; Aldrich and Stevens,

Address reprint requests to Dr. H. A. Fozzard, Cardiac Electrophysiology Laboratories, Box 440, The University of Chicago, 5841 South Maryland Avenue, Chicago, IL 60637.

J. GEN. PHYSIOL. © The Rockefeller University Press · 0022-1295/90/03/0411/27 $2.00
Volume 95 March 1990 411–437

1987). Several aspects of single-channel behavior are not well represented by the Hodgkin-Huxley model of Na current kinetics and alternative Markov chain models have been suggested (French and Horn, 1983). Single Na channel measurements have been used to extract rate constants for some Markovian models by a maximum likelihood method (Horn and Vandenberg, 1984) and by histogram analysis (Kunze et al., 1985; Aldrich and Stevens, 1987). While the choice of the number of channel states and of their configuration remains somewhat arbitrary, it is an effective way to describe channel kinetics and to determine the classes of kinetic models that fit the data most closely.

Although cardiac Na channels have been shown to have many properties similar to those reported for nerve cells (Cachelin et al., 1983; Grant et al., 1983; Kunze et al., 1985; Patlak and Ortiz, 1985; Grant and Starmer, 1987), cardiac Na current kinetics are slower, and decay occurs with more than one time constant (Brown et al., 1981; Grant and Starmer, 1987; Makielski et al., 1987; Kirsch and Brown, 1989). Kunze et al. (1985) demonstrated reopening of the cardiac Na channel and suggested that this property might be responsible for the slow phase of current decay. This seemed plausible since in cells of the neuroblastoma N1E115 cell line current decay has been well described by a single exponential and Na channels usually opened only once in response to a depolarizing step (Aldrich et al., 1983; Aldrich and Stevens, 1987). However, in pituitary GH_3 cells, where current decay has also been well described by a single exponential (Vandenberg and Horn, 1984, Fernandez et al., 1984), Vandenberg and Horn (1984) showed more prominent reopening of the Na channel. A methodological difference that could account for differences between studies of single Na channel kinetics was the use of cell-attached patches (Aldrich et al., 1983; Aldrich and Stevens, 1987) vs. outside-out patches (Horn and Vandenberg, 1984; Vandenberg and Horn, 1984). Horn and Vandenberg (1986) have suggested that the channel reopening behavior they saw may have been nonphysiological, the result of the detached patch configuration or perhaps of the choice of solutions they used. Alternatively, the GH_3, the N1E115, and the cardiac channels may have intrinsically different kinetic properties. This would not be surprising, since it seems clear that there is structural diversity between Na channels (Noda et al., 1986; Sills et al., 1988; Rogart et al., 1989).

We have studied the opening and closing properties of Na channels in cardiac Purkinje cells near threshold and at more depolarized potentials using cell-attached patches. Multichannel patches showed prominent evidence of channel reopening in the threshold voltage range, and this was confirmed by recordings from a patch with a single channel. Inactivation without opening was also prominent near threshold, and both phenomena decreased with depolarization. Mean open duration was a biphasic function of voltage. The single and multichannel patch data were analyzed by the fitting of data histograms (Aldrich and Stevens, 1987) and by a maximal likelihood statistical method similar to that of Horn and Lange (1983). A Markovian kinetic model of the sort used by Horn and Vandenberg (1984) and Kunze et al. (1985) was compatible with the observed channel reopening rates and with the mean open durations. The voltage dependence of the rate constants extracted by the maximum likelihood method were intermediate between those reported by Horn and Vandenberg (1984) and those of Aldrich and Stevens (1987). Although

the model used in this analysis provided the opportunity to compare results with the reported GH_3 and N1E115 data, it consistently underestimated the peak of the probability density functions and predicted less voltage sensitivity of the probability of being open at the peak of the current than was observed experimentally. It also lacked sufficient complexity to produce the observed slow phase of current decay seen with cardiac Na current. This characteristic will require a more complex model, perhaps with additional inactivated states, including one that is not directly in the activation sequence, like that proposed by Chiu (1977). Evidence for the presence of more than one kinetic population of Na channels, as suggested by Benoit et al. (1985), was not found. Some of the results reported here have been previously published in abstract form (Scanley et al., 1985).

METHODS

Preparation of Single Cells

Canine cardiac Purkinje cells were isolated by the method of Sheets et al. (1983). Briefly, free-running Purkinje strands were dissected from canine hearts, cut into small pieces, and incubated at 37°C for 3–4 h in Eagle's minimal essential medium (MEM) (Gibco, Grand Island, NY) containing 5 mg/ml of Type I collagenase (Worthington Biochemical Corp., Freehold, NJ), 0.1 mM free Ca (by addition of EGTA), 5.6 mM Mg, and 1 mg/ml albumin at pH 6.2. Strands were then washed in K-glutamate and briefly homogenized at low speed to separate them into single cells. The cells were stored in MEM. The yield of rod-shaped, calcium-tolerant cells varied between 40 and 90%. The cells providing the best seals were those with well-defined membranes and clear striations.

Experimental Procedure

The preparation of pipettes and the electronics have been described previously (Scanley and Fozzard, 1987). Briefly, the pipettes were double pulled and the tips were coated with Sylgard 184 (Dow Corning Corp., Midland, MI). Pipettes were filled with 140 mM NaCl, 5.4 mM KCl, 1.8 mM $CaCl_2$, 1.0 mM $MgCl_2$, and 10 mM HEPES (pH 7.4). In two patches (10/10A and 10/10B) NaCl was 280 mM, in order to increase the signal-to-noise ratio and to permit accurate measurements at more depolarized voltages. The cell containing the single-channel patch was bathed in the same solution with the addition of 10 mM glucose at 13°C. For purposes of comparison, holding and step potentials for this patch were adjusted by −30 mV, which was a resting potential obtained with fine-tipped microelectrodes (Sheets et al., 1983). Other cells contributing to the data reported here were bathed in 150 mM KCl, 1.0 mM $MgCl_2$, 10 mM glucose, and 10 mM HEPES (pH 7.4). Resting potential for these cells was assumed to be 0 mV and no correction was applied to the holding or step potentials.

A Dagan Corp. (Minneapolis, MN) 8900 Patch Clamp was used with either a Dagan 8930 headstage or a headstage built according to a custom design of Drs. J. Rae and R. Levis (Rush Medical School). The signal was filtered at either 1 kHz using a 2-pole filter for the recordings shown from the single-channel patch (Dagan 8930 headstage) or at 2 kHz using an 8-pole Bessel filter (902-LPF; Frequency Devices, Inc., Haverhill, MA) for all other data (using the custom headstage). Baseline noise, fitted with a Gaussian function, had a standard deviation (σ_n) of 0.12 pA for the custom headstage at 2 kHz and 0.14 pA for the Dagan headstage at 1 kHz. This resulted in a signal-to-noise ratio (A_o/σ_n) of 7–8 for the single-channel patch and 8–15 for the other data shown. All recordings were made in the cell-attached mode with seal resistances of 40–70 GΩ. Voltage control was imposed from an IBM microcomputer

using software written by one of the authors (B. E. Scanley). Membrane patches were depolarized to test potentials for 45 ms once per second from holding potentials between −100 and −140 mV. A capacity compensation circuit was used to reduce the capacity transient. Data were acquired at 10 kHz and stored on floppy disk for analysis.

Data Analysis

Further capacity correction and leak subtraction was accomplished by averaging sweeps without openings at a given potential and subtracting this from sweeps with activity. Single-channel opening events were defined as currents that exceeded half the average open-channel current amplitude. Dead time for data filtered at 1 kHz was 178 μs and at 2 kHz it was 90 μs (Colquhoun and Sigworth, 1983); events shorter that these dead times would not be detected. The fraction of missed events was estimated from the open-time distributions as (*a*) the relative area under the exponential function describing the open-time histogram between zero and dead time, and (*b*) the difference between the detected events in the first bin and the number predicted for the first bin by the exponential function. These gave comparable estimates, although the latter technique sometimes predicted a larger number of missed events. Suppression of false openings due to noise was enhanced by requiring that two sample points be recorded above threshold for recognition of an event, although this increased the number of missed events. When more than one channel was open at a time, threshold was set at half the amplitude plus a multiple of the average open-channel current amplitude. Patches having sweeps with more than four simultaneous openings were not analyzed, and occasional sweeps were deleted because of noise artifacts. Histogram analysis was carried out on a Masscomp 5520 microcomputer using a modified Gauss-Newton nonlinear regression algorithm from the Numerical Algorithms Group (NAG) library. Because of missed short events, open time histograms were fitted after exclusion of the first (0.5 ms) bin.

Model Analysis

A maximum likelihood method was used to compare predictions of Markov chain models with experimental recordings. The model chosen was the basic five-state model used by Horn and Vandenberg (1984) and is schematically presented below:

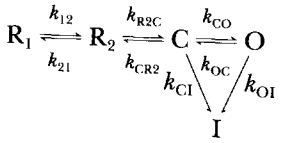

(Scheme 1)

States R_1, R_2, and C are closed, rested states. O is an open state and I is a closed, absorbing, inactivated state. The maximum likelihood method used was a modification of the method developed by Horn and Lange (1983). It involved developing a likelihood function that described the probability of observing a specific set of experimental recordings. This equation was derived first from the construction of probability density functions (PDFs), which used the transition rate constants to describe the probability of observing each of the possible state transitions as a function of time. A likelihood function was then constructed for each experimental sweep using the PDFs and the observed transition times (open/closed times) such that the function described the probability of observing that individual record. Finally, because each sweep was assumed to be independent from the others, the likelihood function for all of the sweeps at one step potential was determined as the product of all of the individ-

ual likelihood functions. The transition rate constants were then derived by finding those values of the rate constants for which the likelihood function was at its maximum. The Q-matrix method of Colquhoun and Hawkes (1977) was used to develop the PDFs for each of the kinetic transitions allowed within the model. Determination of the initial state distribution is subject to significant error and this is discussed below. Patches with more than one channel were also analyzed with this method. Each sweep in a patch with n channels was analyzed as being equivalent to an ensemble of n sweeps from a single-channel patch. The maximum likelihood analysis used the mathematical libraries of NAG and IMSL and computation was performed using a University of Pittsburgh VAX and the CRAY X-MP/48 in the Pittsburgh Supercomputer Center and the CRAY X-MP/24 in the San Diego Supercomputer Center. For further details see Chay (1988).

RESULTS

Channel Reopenings

Although channel reopening can be suspected from recordings of patches containing several channels (e.g., Kunze et al., 1985), uncertainty as to the number of channels in the patch renders detailed analysis difficult. One patch in the present study contained only one Na channel, and its recording permitted unequivocal evaluation of reopening. A comparison with data from 14 multichannel patches showed that the behavior of the single channel was similar to that of channels in other patches.

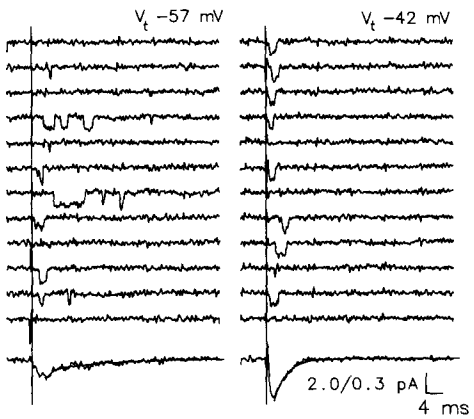

FIGURE 1. Recordings of openings in the single-channel patch. Sequential recordings are shown of channel openings. Data were filtered at 1 kHz and recorded with the Dagan headstage. See Methods for experimental conditions. Voltages are reported including the cell resting potential, which was estimated to be −30 mV. Records on the left show recordings for steps to −57 mV and on the right threshold steps to −42 mV from an estimated holding potential of −120 mV. Note that there are traces with no openings (nulls) and others with several reopenings. The lower part of the figure shows ensembles of the single-channel currents representing averages of sweeps with activity including 100 sweeps at −57 mV and 357 sweeps at −42 mV. Exponential fits to the decay of the ensemble currents are shown. At the more negative potential two exponentials fitted better than one with τ_1 = 1.0 ms and τ_2 = 12.6 ms. At −42 mV a single exponential fit was best with τ = 2.9 ms.

Evidence that the patch contained only one channel is based upon the absence of observing any double amplitude openings in 1,998 sweeps and a maximum likelihood probability estimate based upon the method of Patlak and Horn (1982). Estimates of the probability that there could have been two channels were made at three step potentials (−57, −47, and −42 mV) with the greatest number of sweeps

(1,144 sweeps containing 758 openings). Probabilities were 0.20, 0.02, and 0.0001 for the three voltages, respectively. The lower estimate for the more depolarized potential is the result of a greater number of sweeps obtained at that voltage and the more condensed time course of the probability density function for the open state.

Examples of sequential recordings of voltage steps in the single-channel patch are shown in Fig. 1. Repetitive openings were seen at the more negative step potentials. Reopening behavior was stable over the time period of data collection. The distribu-

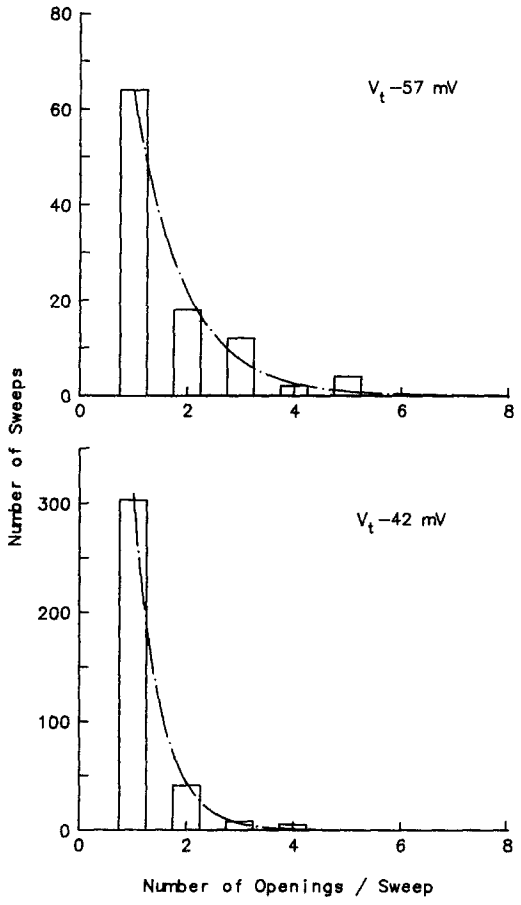

FIGURE 2. Number of openings per sweep. Histogram of numbers of openings in each step depolarization with activity from the single-channel patch. Most sweeps contained only one opening, and the numbers of openings per sweep declined exponentially. The upper and lower panels show data for steps to −57 and −42 mV, respectively. Note that reopenings were less frequent at −42 mV.

tions of the number of openings per sweep at −57 and −42 mV are shown in Fig. 2. The monoexponential decay indicates that during these recording periods the channel did not enter a reopening or burst "mode" during which there were a disproportionate number of openings. The frequency of reopenings was strikingly voltage dependent (Fig. 3). Sweeps recorded near threshold voltage showed the largest number of reopenings. At −57 mV there were 164 opening events in 100 sweeps with activity, such that 39% of opening events at that voltage were reopenings. The

number of reopenings may be somewhat underestimated because of brief openings missed as a consequence of the filter frequency (1 kHz in this patch). Missed brief events were estimated to be 5–15% based on calculations of dead time and comparison of detected events with the exponential function fit of the open-time histograms. The error introduces a scaling factor (Kunze et al., 1985), without significant distortion of the shape of the relationship in Fig. 2.

The large number of reopenings at more negative potentials offered the opportunity to examine closed intervals at several voltages (Fig. 4). Brief closures could not be determined accurately because of the filter cutoff. A calculation from the closed interval histogram of the number of missed closures of full amplitude based on filter-induced dead time and probability of reopenings within that time from the closed interval histogram resulted in an estimate of one to three missed events per second of channel open time for −57 mV and less than one per second of channel open time for −42 mV (Colquhoun and Sigworth, 1983). The closed duration distributions were well described by single exponentials, consistent with reopening

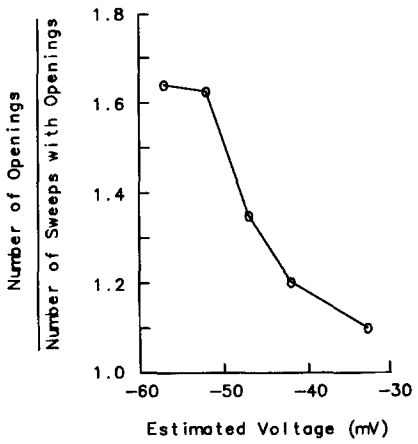

FIGURE 3. Voltage dependence of reopening. Reopenings were calculated as the total number of openings divided by the number of sweeps with openings plotted as a function of step potential. The data are from the single-channel patch.

occurring predominantly from one channel state. The slight excess of long closed intervals could have resulted partly from missed openings in those intervals (estimated to be 5–10%), but the small size of the data set prevented us from excluding a more complex reopening pattern. The closed duration data were also subject to some error because of false events, which result when random noise is classified as openings or closings. These were estimated to be $<1\ s^{-1}$ for these data (Colquhoun and Sigworth, 1983).

Open-Channel Durations

The distribution of the times spent in the open state provides information about the possible number of open states and the rates of channel closure. Prior reports of open durations for cardiac Na channels have indicated that the distribution is well described by a single exponential (Grant et al., 1983; Patlak and Ortiz, 1985; Kohlhardt et al., 1986; Fozzard et al., 1987), although Kunze et al. (1985) and Nagy (1987) reported biexponential distributions. Open durations were examined in 14

patches at different voltages (45 fits). They were well fitted by single exponentials with mean open durations between 0.5 and 1.9 ms. Examples of histograms of open durations and the exponential fits are shown in Fig. 5. Exceptions to the single exponential distribution of open durations occurred only when very long openings were observed (Fozzard et al., 1987). These represented <1% of the openings and were thought to be similar to those reported by Patlak and Ortiz (1985) and Kiyosue and Arita (1989).

The determination of open duration in multichannel patches is subject to error when openings overlap. Open durations are biased towards shorter values when

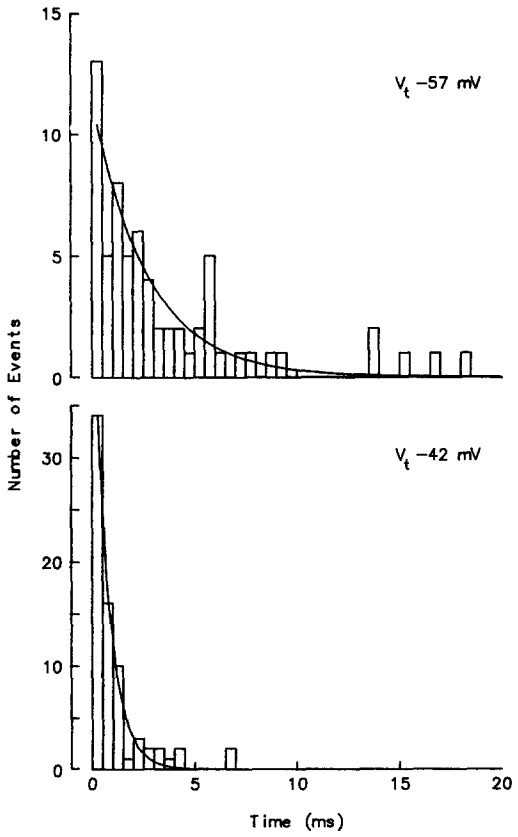

FIGURE 4. Closed intervals. Intervals between the time of closing and reopening were measured in sweeps in which reopenings occurred. The data are from the single-channel patch. Closed intervals shortened with depolarization. The histograms were well fitted with one exponential, although at the more negative potential there was an excess of long closed intervals suggesting a small slower component. τ at −57 mV = 2.7 ms; τ at −42 mV = 0.7 ms.

overlapping events are excluded from the analysis or when duration is calculated always assuming the first closure in overlapping events belongs with the first opening (pairing). To reassure ourselves that pairing did not influence open duration analysis, we compared calculations from the histogram analysis in the multichannel patches, where open durations from overlapping openings were calculated by pairing first openings with first closings, with those from the maximum likelihood calculations, where openings were randomly paired with closings in overlapping events to calculate open duration. Mean open durations were also estimated from the maximum likelihood calculations of the rate constants for the two exit paths from the

open state. The mean open durations obtained by the two methods were not significantly different (see Fig. 13). Open durations in the single channel patch were free of overlapping events and examination of these data confirmed the single exponential distribution predicted by a first order process (Fig. 6).

To confirm that the open durations did not change during a sweep, we divided each sweep into two parts at the time at which half of all of the events had occurred. The open duration distributions were not significantly different for the earlier

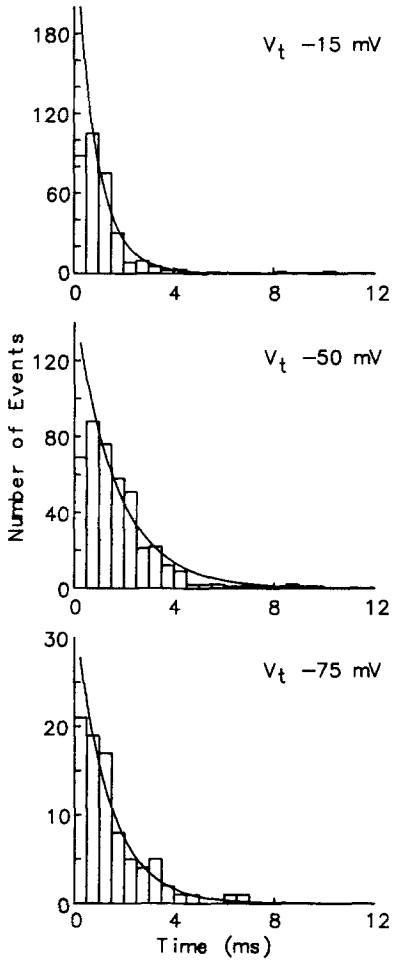

FIGURE 5. Open-duration histograms. This patch (10/3A) had an estimated four channels. Data were filtered at 2 kHz and recorded with the custom headstage. See Methods for experimental conditions. Single exponential fits yielded time constants of 0.8 ms (−15 mV), 1.7 ms (−50 mV), and 1.4 ms (−75 mV). The first bin was excluded from the fits.

openings compared with the later openings. We also examined the open durations of the reopenings and found no difference from the first openings. Because of the filter some brief openings were undetected. However, the first bins of these histograms were larger than the dead times so that their omission during the fitting process should have minimized error from this cause in estimation of the mean open times.

The voltage dependence of the mean open durations was examined for four

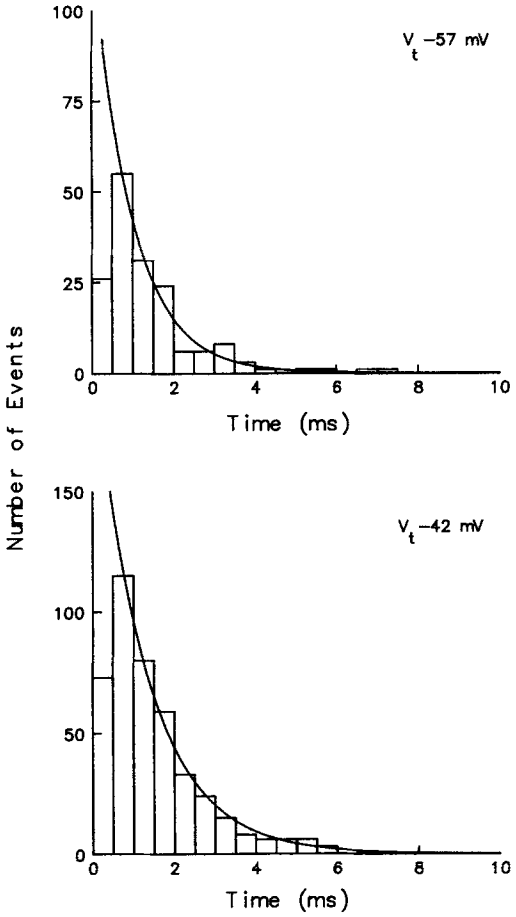

FIGURE 6. Open durations in the single-channel patch. The two panels show histograms taken from steps to −57 and −42 mV. Single exponential fits yielded time constants of 1.0 ms at −57 mV and 1.3 ms at −42 mV. The first bin was excluded from the fits.

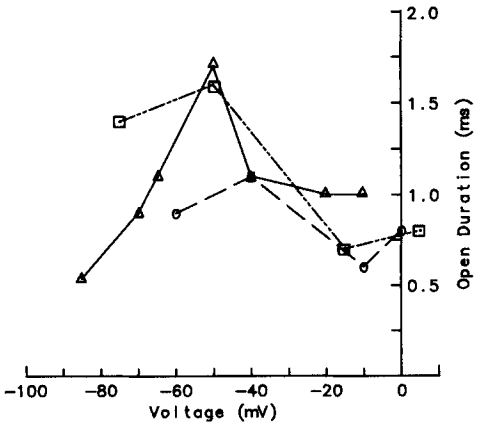

FIGURE 7. Voltage dependence of mean open durations. Three patches had mean open durations determined at several test voltages. Although there was some scatter, the mean open durations have a biphasic dependence on step potential. Patches 10/3 A (□), 10/10 A (○), and 10/10 B (△).

patches in which a sufficient voltage range of data was available (Fig. 7). At potentials of −65 mV and more negative, the mean open duration averaged 0.9 ± 0.1 ms, increased to 1.3 ± 0.1 ms at potentials of −50 to −40 mV, and became shorter again (0.8 ± 0.1 ms) at more depolarized potentials. The mean open duration in a single open state is described by the inverse of the sum of rate constants leaving the open state $(k_{OC} + k_{OI})^{-1}$. The biphasic dependence of open durations on voltage is consistent with a model containing two exit paths from the open state with opposite monotonic voltage dependence (See Aldrich and Stevens, 1987, for further discussion).

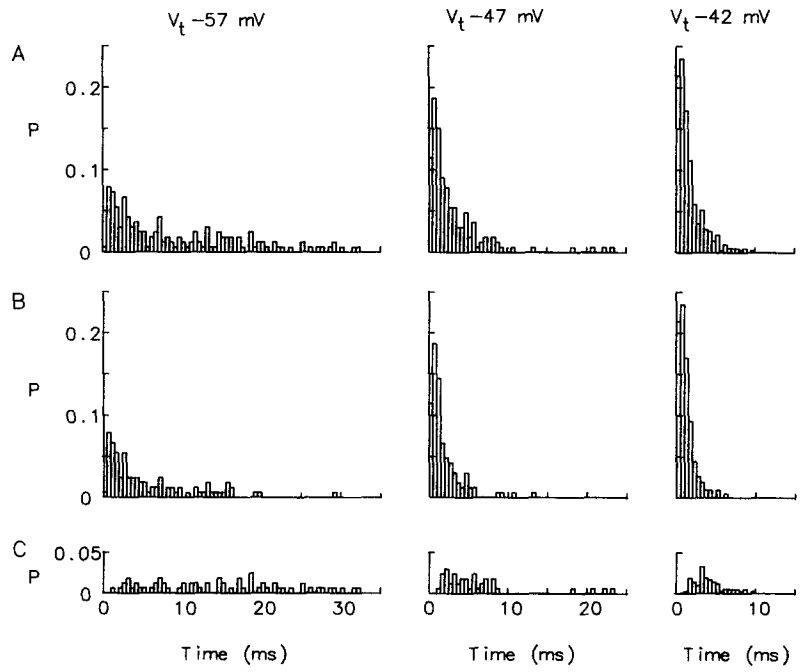

FIGURE 8. Waiting times for the single-channel patch. Data are shown for three voltages. The scale is the same for the three voltages. (*A*) Waiting times to all openings. At −57 mV the peak probability of opening was quite slow and the openings were spread over 20–30 ms. (*B*) Waiting time to first opening. The same pattern of voltage dependence as for all waiting times is seen. (*C*) Waiting time to reopenings (all latencies–first latencies). Significant numbers of reopenings occur at negative step potentials.

Waiting Times and Ensemble Currents

The first-latency, all-latency, and difference histograms for the single-channel patch are shown in Fig. 8. The all-latency histograms at −57 and −47 mV were better fitted with two exponentials than with one, which is consistent with the presence of the two time constants of current decay at these potentials. The fit for −57 mV is shown in Fig. 1. It was also possible to fit the declining phase of the first-latency distribution at these two potentials with either one or two exponentials (not shown),

but discrimination could not be made between the two functions. Reopening histograms in the lower part of the figure show the difference between the all-latency and first-latency histograms. They demonstrate the extent to which reopening contributes to the decay component of the current at step potentials near threshold. All of the latency histograms demonstrated an early rising phase. This is attributable to the presence of multiple closed states prior to the open state, but since data in this early time period were subject to uncertainty because of the duration of the capacity transient, they were not quantitatively analyzed.

Failure to Open

At every voltage examined for both the single-channel patch and those containing several channels, some steps failed to elicit any observable channel openings. Fig. 9 shows the null probability (P_N) as a function of voltage for the single-channel patch, and Fig. 10 shows the P_N for four multichannel patches bathed in KCl, normalized

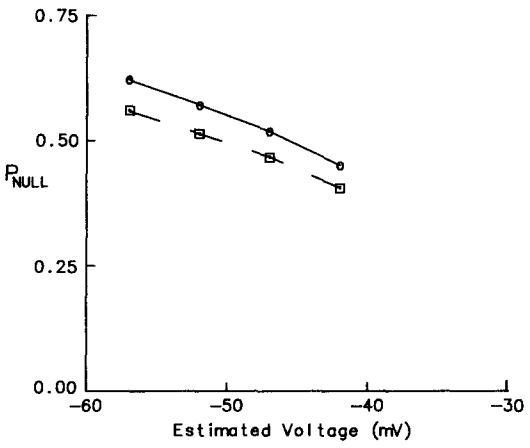

FIGURE 9. Voltage dependence of nulls. The fraction of sweeps that were without openings is plotted against step potential for the single-channel patch (○). These can be thought to primarily represent the fraction of sweeps in which the channel inactivated directly without entering the open state, if it is assumed that it was never in the inactivated state at the time of the step. If the channel were already inactivated 10% of the time, the curve would be displaced downward, as shown (□), in order to represent accurately the number of sweeps in which the channel inactivated without opening.

by taking the n^{th} root of the fraction of observed null sweeps (where n equals the estimated number of channels in the patch). There was in all cases a decline in nulls with depolarization.

Nulls are considered to occur by inactivation of the channel directly from the closed state without entering the open state (Horn et al., 1981). However, three alternative possibilities exist that could cause nulls to overestimate P_N and at least one that would cause underestimation: (*a*) an opening occurred that was too brief to be detected, (*b*) an early opening occurred that was obscured by the capacity transient, (*c*) channels were already in the inactivated state at the time of the step, or (*d*) the channel remained in closed, noninactivated states throughout the step. Estimates of missed brief events were predicted from mean open duration and filter characteristics (discussed above) and these varied from 5–15%, being largest at those potentials at which the mean open time was the shortest. The capacity transient is especially problematic at positive potentials where first latency is short. Data

from the most depolarized potentials for the multichannel patches were omitted in Fig. 10 because at those voltages activation encroached on the capacity transient, making estimation of the number of null sweeps unreliable.

The solid line in Fig. 9 shows the fraction of sweeps during which the channel inactivates without opening if, at the beginning of every depolarization, the channel was assumed to be in a rested, noninactivated state. If, however, 10% of the time the channels were already in the inactivated state, the dashed line would describe the voltage dependence of inactivation without opening. On the other hand, if some channels never left the closed, noninactivated states, the relationship would be shifted in the opposite direction.

The probability of inactivating without opening is principally determined by the relationship of the rate constants from the closed to open state (C → O) and from

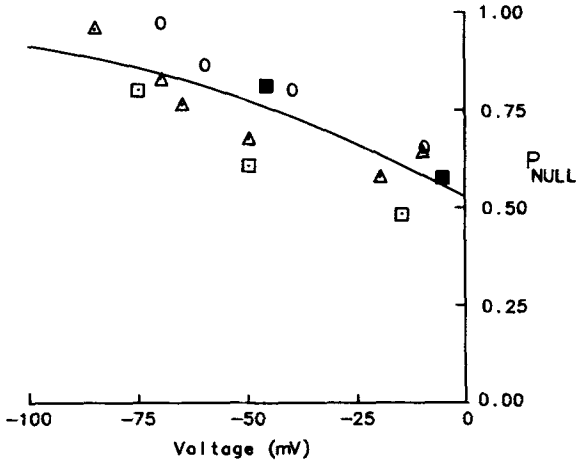

FIGURE 10. Derived null fraction for multichannel patches. Data for four patches with two to four channels were analyzed for nulls by taking the n^{th} root of the observed fraction of nulls, where n is the number of channels estimated by the maximum likelihood method. There is a modest decline in percent nulls with depolarization. The line is a nonlinear least-squares fit to a simple Boltzmann with $V(1/2)$ = 4 mV and slope = 44 mV. See text for discussion. Patches 10/10A (○), 10/10B (△), 10/3A (□), and 4/11D (■) with estimated numbers of channels in each patch of 4, 4, 4, and 3, respectively.

the closed to the inactivated state (C → I), at least over the potential range at which the rate of return to previous closed states is low. Of course, at hyperpolarized potentials P_N reaches 1.0 not only because the C → O transition rate is low, but because channels remain in previous closed states. However, if one assumes the primary determinant of P_N is the probability of inactivating without opening, then P_N is equal to $k_{CI}/(k_{CI} + k_{CO})$. If further, C → O and C → I transition rates are simple exponential functions of voltage, then the P_N-voltage relationship will be described by a simple Boltzmann, the slope of which will be determined by the relative voltage dependence of the k_{CI} and k_{CO} transition rates. The line in Fig. 10 is the Boltzmann fit to the multichannel patch data and predicts a slope of 44 mV, or about one-half e^-. The slope for the single-channel patch (Fig. 9) appears steeper (20 mV) than that for the multichannel patches (Fig. 10), and the overall frequency of null sweeps was

less. This patch was studied at 13°C and other patches at 10–12°C (see Discussion).

Choice of Model

The histogram analysis suggested that Markov chain models similar to those used by Horn and Vandenberg (1984), Aldrich et al. (1983), and Kunze et al. (1985) are appropriate for analysis of Na channel behavior in cardiac Purkinje cells. Model features that were indicated from the data included the following: (*a*) The delay in peak frequency of opening in the first-latency histograms was consistent with several closed states before the channel opens. (*b*) The single exponential open-duration distribution agreed with the conclusion of Horn and Vandenberg (1984) that there is only one open state. (*c*) The reopening seen in the single-channel patch required oscillation between the open state and one or more adjacent closed states before inactivation. (*d*) The closed interval distribution was consistent with these oscillations being predominantly from one state, without ruling out a second closed state. (*e*) The occurrence of null sweeps required a path to inactivation that bypassed the open state. (*f*) Many of the ensembles and all latencies histograms demonstrated a second, slowly decaying component, which suggested models such as those containing a nonabsorbing closed state just before the absorbing, inactivated state (e.g., Chiu, 1977).

These characteristics, with the exception of the slowly decaying component of the latency distribution, are reproduced by the basic five-state model of Horn and Vandenberg (1984). We chose this model because the size of the slow component was too small to determine the extra parameters with accuracy. We used a maximum likelihood method to analyze our data (see Methods) and compared the results with the histogram analysis. Data analyzed in histogram form may lose some of the relational information present in the original data, and these relations are preserved in the maximum likelihood method. The maximum likelihood analysis also provides standard errors of the estimate for fitted parameters, which helps in evaluating the reliability of the estimates. However, the two analysis methods represent important checks on each other because of their inherently different sources of error. The maximum likelihood analysis was first applied to data from the single-channel patch and then extended to multichannel patches.

Several assumptions were tested in the analysis. (*a*) The assumption that the I state acts as a sink at depolarized potentials was tested by allowing finite return rates from the I state (k_{IO} or k_{IC}). The model fits indicated that these rates approached zero at all voltages tested, so all results reported here used the assumption that I represented an absorbing state. (*b*) The computation required assignment of probabilities that the channel was in each of the closed states just prior to depolarization. Maintenance of a negative holding potential assured that the probability of being in the I state was small. Computations assumed that the $P(\mathrm{I}) = 0.1$, but other choices would not have changed the results since I was an absorbing state. Assumptions of the initial distribution of the probabilities of being in states R_2, R_1, and C affected the rising phase of the function describing the probability of the channel being open. However, the experimental data in that initial time period were not considered sufficiently reliable to determine this initial distribution because of the duration of the

capacity transient. Although the arbitrary initial state distributions made the closed state transition rates unreliable, they had little effect on the other transition rates (see Discussion).

Predictions of the Model

Table I shows the transition rates calculated at four voltages from the single-channel data using the five-state model illustrated in the Methods. The transition rates determined by the maximum likelihood method from the single-channel patch were used to calculate the open probability function, $P_{open}(t)$ (Fig. 11). The fits were satisfactory across this voltage range, except that the predicted peak in $P_{open}(t)$ was in each case somewhat lower than that observed. However, the time to peak of the data was predicted well.

Predictions of the model for the number of openings per sweep for the single-channel patch are shown in Fig. 12. Agreement with the observed number of null

TABLE I

k	−57 mV	−52 mV	−47 mV	−42 mV
		ms^{-1}		
R_1R_2	0.30 ± 0.15	0.35 ± 0.12	6.52 ± 5.58	7.734 ± 2.64
R_2C	2.70 ± 1.83	6.95 ± 6.14	5.99 ± 5.23	4.29 ± 1.40
CR_2	0.47 ± 0.47	0 ± 2.32	0 ± 2.80	0 ± 0.79
CI	0.24 ± 0.05	0.26 ± 0.10	0.26 ± 0.13	0.87 ± 0.09
	(0.24)		(0.35)	(0.68)
CO	0.18 ± 0.04	0.28 ± 0.10	0.29 ± 0.15	0.64 ± 0.14
	(0.15)		(0.32)	(0.83)
OC	0.70 ± 0.10	0.53 ± 0.12	0.35 ± 0.06	0.18 ± 0.02
	(0.8)		(0.52)	(0.29)
OI	0.05 ± 0.09	0.13 ± 0.11	0.37 ± 0.06	0.51 ± 0.03
	(0.24)		(0.31)	(0.49)

Rate constants and standard error of the estimates for maximum likelihood fits to the five-state model described in the Methods for the patch with one channel (1/29). Numbers in parentheses are the rate constants calculated from the histogram measurements (see text).

sweeps and the number of reopenings was good. Similar agreement occurred with three multichannel patches analyzed by the maximum likelihood method (10/3A, 10/10A, and 10/10B). This agreement shows that the model was sufficient to reproduce both reopenings and failure to open of the cardiac Na channel, as was also shown by Horn and Vandenberg (1984) for GH_3 cells. Although reopenings most likely contribute to the slow decay phase of the all-latencies distribution, this analysis showed that reopenings were also important in their contribution to the time course of the rapid initial decay of the all-latencies distribution.

The open-duration distribution according to the model is described by a single time constant equal to $(k_{OI} + k_{OC})^{-1}$. The maximum likelihood calculations compared well with the mean open duration values determined by histogram analysis for the single-channel patch and three multichannel patches. For example, for the patch shown in Fig. 5 (10/3A), the maximum likelihood calculations predicted open durations of 0.8 ms at +5 mV (compared to 0.8 ms obtained by exponential fits to

the open-duration histogram); 1.1 ms at −15 mV (compared with 0.8 ms), 1.6 ms at −50 mV (compared with 1.7 ms), and 1.4 ms at −75 mV (compared with 1.4 ms). The voltage dependence of mean open time derived for maximum likelihood calculation was bell-shaped (Fig. 13), as was the histogram-derived data shown in Fig. 7.

Closed intervals, illustrated in Fig. 4, were also compared with the rate constants derived from maximum likelihood calculations. In the model, closed intervals are

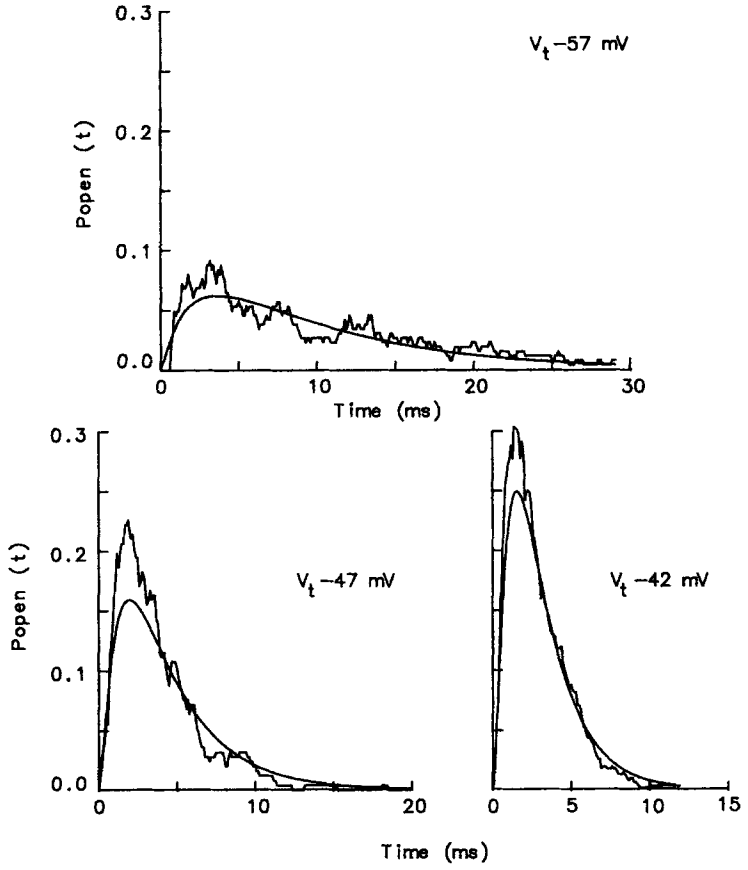

FIGURE 11. Comparison of the observed probability of the channel being open with that predicted by the maximum likelihood analysis. The data are the all-latency histograms convoluted with the mean open times. The data are from the single-channel patch at −57, −47, and −42 mV.

exponentially distributed with time constants of $(k_{CO} + k_{CI})^{-1}$, providing k_{CR2} is small (Vandenberg and Horn, 1984). For the single-channel patch, sufficient reopenings occurred to permit the estimation of the time constant of a single exponential fit. For −57 mV the histogram fit yielded τ equal to 2.7 ms, compared with the computed τ of 2.4 ms. At −47 mV the histogram τ was 1.5 ms and the computed τ was 1.8 ms. At −42 mV the histogram τ was 0.7 ms and the computed τ was 1.0 ms.

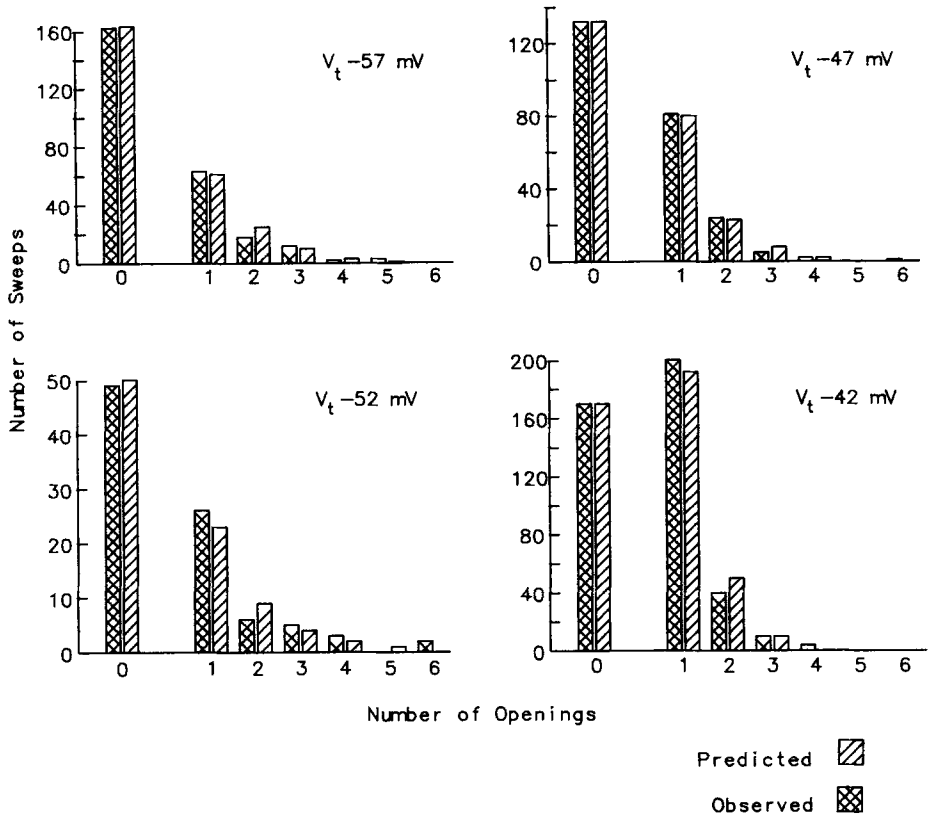

FIGURE 12. Observed frequency of openings per sweep compared with that predicted by maximum likelihood analysis for the single-channel patch. The voltage dependence of reopening and of null sweeps is apparent and well matched by the model.

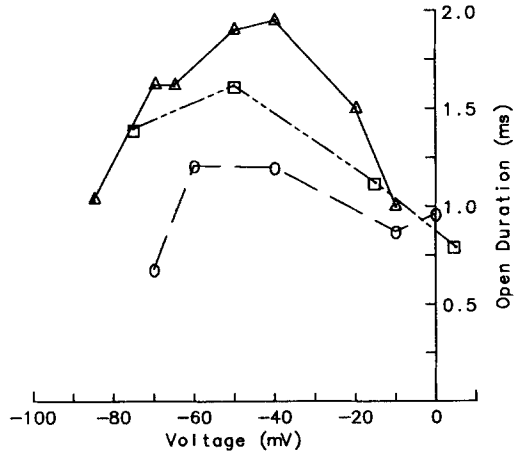

FIGURE 13. Voltage dependence of open-channel duration as predicted by the maximum likelihood analysis. Patches 10/10A (O), 10/10B (△), and 10/3A (□).

The probability of inactivation without opening was high at negative potentials, because k_{CI} is larger than k_{CO}. However, k_{CO} increases more rapidly with depolarization, increasing the relative probability of opening. Reopening is a consequence of return from the open state to the closed state, in preference to progression to the absorbing state, because near threshold k_{OC} is similar to k_{OI}. With depolarization, k_{OC} falls rapidly relative to k_{OI}, so transitions from open to closed become rare. The same properties are consistent with the biphasic mean open-time dependence on voltage. Initially, the mean open time is prolonged with depolarization because k_{OC} falls. With further depolarization, the increase in k_{OI} reduces the mean open time.

The characteristic voltage-dependent behavior of the Na channel, as modeled by the Markov chain, is the consequence of the voltage dependence of the various transition rates. Rate constants obtained from maximum likelihood analysis of four patches are shown plotted against membrane potential in Fig. 14. In an effort to obtain the best estimate of the slopes of the relationships, weighted log-linear regressions were calculated with the constraint that the data from each patch be fitted with a line of the same slope, while allowing variation in the intercepts. In general the grouped data exhibited lesser voltage dependence of the rate constants than did the fits to the single-channel patch data alone. The voltage dependencies of the rate constants k_{CO} and k_{OC} were opposite in sign and similar in magnitude; each showed an e-fold change with a depolarization of ~30 mV, equivalent to just under one electron charge crossing the membrane field. k_{OI} decreased with depolarization, also with a rate equivalent to just less than one charge. k_{CI} increased with depolarization with a smaller slope equivalent to about one-half charge. Voltage dependencies of closed state transitions, $R_1 \rightarrow R_2$ and $R_2 \rightarrow C$, were 1.4 e^- and 0.7 e^-.

The largest errors in the estimates occurred with the closed-state transition rates (Fig. 14, *top*), while other estimate errors were much smaller except when, as for the $O \rightarrow I$ transition, rates were very slow. To assess the effect of the choice of the model on the predicted transition rates and their voltage dependency, we compared the estimates for the single-channel patch data alone with the five-state model with fits to two simpler models with only one rested state, in which entry to the inactivated state occurred only from either the rested state or the closed state.

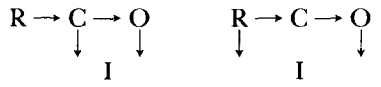

(Scheme 2)

Voltage dependencies of rates to and from the open state, k_{CO}, k_{OC}, and k_{OI}, were insensitive to the choice of the model. The magnitude and the sign were in all cases essentially identical and about twice that predicted from the grouped data (Fig. 14). As might be expected, however, estimates of rates of the closed-state transitions were much more sensitive to model choice. Both of the simpler models predicted k_{RC} to have a similar voltage dependence of 2 e^-. This was in contrast to the fit of the single-channel data alone to the five-state model where k_{R1R2} was predicted to be steeply voltage dependent (6 e^-) and k_{R2C} was predicted to have no voltage dependency. Additional certainty as to the voltage dependency of these rates was perhaps gained by grouping the single-channel patch data with the multichannel data (Fig. 14). The rate of inactivation without opening was the most interesting in that opposite dependency upon voltage was predicted for k_{CI} (−1.2 e^-) and k_{RI} (1.5 e^-) rates

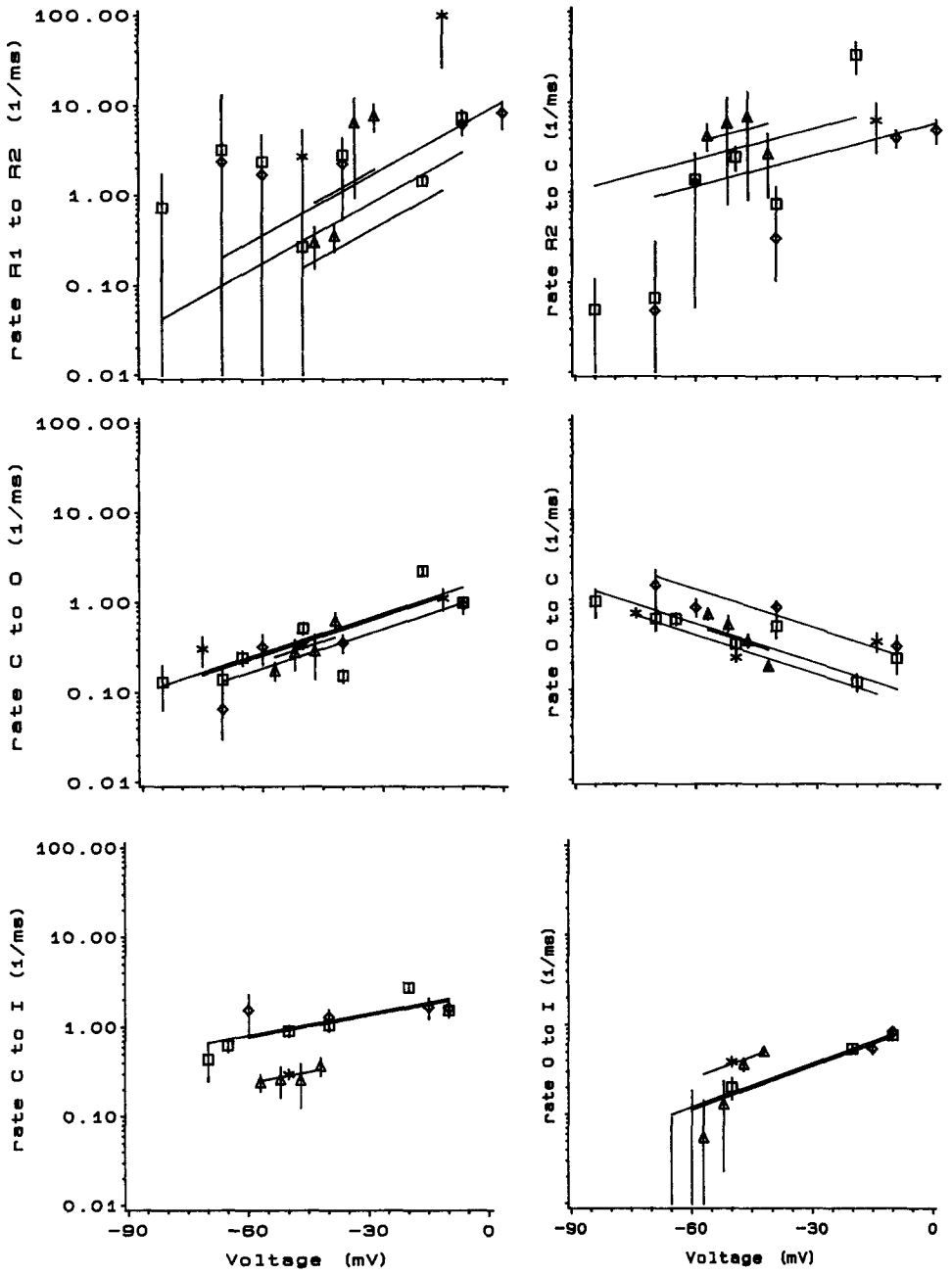

FIGURE 14. Voltage dependence of rate constants. Weighted linear regressions of the maximum likelihood estimates for the five-state model described in the Methods, constraining data from each patch to the same slope. Fitted lines gave e-fold changes in the rate constants as follows: for $R_1 \rightarrow R_2$ (k_{R1R2}), 20 ± 6 mV; for $R_2 \rightarrow C$ (k_{R2C}), 37 ± 7 mV; for activation from $C \rightarrow O$ (k_{CO}), 30 ± 6 mV; for inactivation from $C \rightarrow I$ (k_{CI}), 53 ± 7 mV; for inactivation from $O \rightarrow I$ (k_{OI}), 27 ± 4 mV; and for closure from $O \rightarrow C$ (k_{OC}), 30 ± 4 mV. Thus, the number of electrons required for each transition were ~ 1.4, 0.6, 0.8, 0.5, 0.9 and 0.8, respectively. Patches 10/10B (□), 10/3A (*), 10/10A (◇), and the single-channel patch, 1/29 (△).

in the fits to the two simpler models. However, for the five-state model the voltage dependence of k_{CI} was predicted to be 0.7 e^-, only slightly greater than the dependency predicted from the grouped data (0.5 e^-).

The values of the four rate constants k_{CI}, k_{CO}, k_{OC} and k_{OI} were also estimated for the single-channel patch from direct experimental measures of mean open time, mean closed time, null frequency, and reopening, following the lead of Aldrich and Stevens (1987) and Horn and Vandenberg (1984). The assumptions for those calculations were that k_{CR} was small at the voltages studied and that departure rate from the closed state after return from the open state was the same as the initial departure rate from the closed state. These calculations yielded rate constants close to

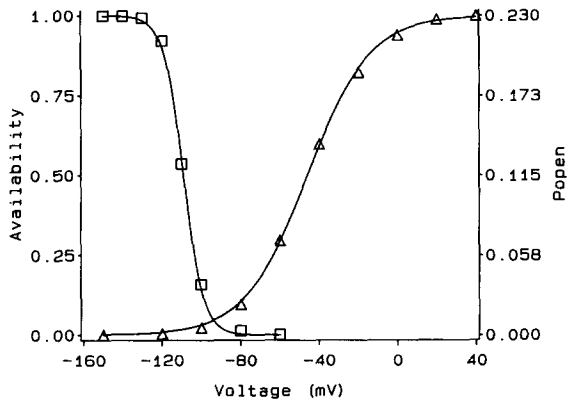

FIGURE 15. Behavior of an "average" channel based on fits to grouped data shown in Fig. 14. Rate constants at 0 mV were estimated as the weighted means of the intercepts in those fits. Probabilities that a channel would be open at the peak of the current in steps to the indicated voltages are plotted as triangles; the line shows the fit of the data to a Boltzmann distribution with a half-point of −46 mV, slope of 16 mV, and plateau value of 0.23. Note that this underestimated the recorded probabilities, as seen for example in Fig. 11 where P_{open} reached 0.3. Back rate constants produced steep voltage dependence of channel availability, graphed as the probability of not being in the inactivated state at the end of 500 ms (□). The line shown is the Boltzmann fit to the data with the half-point at −109 mV and a slope of 5 mV. The relationship was very sensitive to the selection of the backward rates. Shown is the solution when k_{CR2} and k_{R2R1} were given the opposite slope to the corresponding forward reaction and values at 0 mV were set to 0.07 s^{-1} and 30 s^{-1}, respectively. k_{IC} was given a negative voltage dependency of 2.1 e^- and k_{IO} had essentially none (0.1 s^{-1}). Availability was determined by the values given the free parameters and was primarily constrained here by the requirement that fewer than 0.3% of the channels accumulate in the open state at any potential.

those obtained by the maximum likelihood method, and the rate constants had similar voltage dependences (Table I).

Overall Behavior of the Model

The values predicted from the fits to the grouped data (Fig. 14) were used to calculate rates for an "average channel," and the voltage dependence of its behavior was examined (Fig. 15). Estimates for rate constants at 0 mV were calculated as the weighted means of the intercepts from the fits graphed in Fig. 14. The missing backward rate constants were estimated assuming k_{CR2} and k_{R2R1} had the opposite voltage

dependence as the corresponding forward reactions. Backward rate constants for k_{IO} and k_{IC} were estimated using the constraints that the C → O → I loop should be microscopically reversible and the backward rates should be sufficiently slow such that < 0.3% of the channels accumulated in the open state at equilibrium between −160 and 40 mV. Microscopic reversibility required k_{IC} to be about 34 times slower than k_{IO} at 0 mV.

The probability that the "average" channel would be open at the peak of the current during steps to the indicated voltages is plotted as triangles in Fig. 15. The half-point of the relationship matched well those observed in peak conductance curves measured from macroscopic currents at this temperature (e.g., Hanck et al., 1990). However, the slope was considerably shallower, only about half that of macroscopic peak conductance curves. Also, as mentioned above, this probability consistently underestimated the observed probabilities that the channel was open at the peak of the current.

The inclusion of estimates for the back rate constants produced a model with voltage-dependent channel availability. Although the model did not assign a large voltage dependence to inactivation from the closed state (k_{CI}, 0.45 e^-), the distribution of channels between the various nonconducting states was steeply voltage dependent if one assumed the closed-state transitions had the opposite voltage dependence to the forward ones. Fig. 15 graphs the probability that the "average" channel would not be in the inactivated state after 500 ms as squares. This value is essentially equivalent to a measurement of macroscopic steady-state availability as a function of holding potential. Macroscopic I_{Na} measurements in cardiac Purkinje cells (e.g., Makielski et al., 1987) indicate that this relationship is quite steep with a slope between 5 and 6 mV, which matches well the slope produced by the model. However, it should be stressed that this property was determined by the choice of values for the "free" parameters. This was in sharp contrast to the activation relationship which was very insensitive to the choice of the backward rates.

DISCUSSION

The kinetic properties of single Na channel recordings from cardiac Purkinje cells resemble those reported by Horn and Vandenberg (1984) and Vandenberg and Horn (1984) for GH_3 cells, and by Aldrich and Stevens (1987) for N1E115 cells. Our analysis of channel behavior used two methods, conventional histograms and the statistical method of maximum likelihood, to extract rate constants for a Markovian model with five states. These two methods gave similar estimates. Several important kinetic properties of cardiac Na channels were demonstrated: (*a*) Most of the voltage dependence of the cardiac Na channel resided in the activation steps. (*b*) There was striking reopening behavior near threshold, which diminished dramatically at potentials near 0 mV. (*c*) Inactivation from the open state was voltage dependent. (*d*) Inactivation without opening was prominent, and it was also voltage dependent.

As reported by Horn and Vandenberg (1984) and Vandenberg and Horn (1984) for GH_3 cells and by Aldrich and Stevens (1987) for N1E115 cells, activation kinetics were the most important factor in determining the peak and the declining phase

of the current. Inactivation did play an important role as well, although its voltage dependence was less.

Channel Reopening

A single-channel patch offered the opportunity to demonstrate channel reopening behavior directly. Reopening was an important source of Na current for the cardiac cell at voltages near threshold, accounting for as much as 39% of the current. At more depolarized potentials reopening was reduced dramatically, contributing only 5–10% of the current. These data are consistent with predictions from multichannel patch recordings by Kunze et al. (1985) and Kirsch and Brown (1989) in neonatal rat ventricular cells. Our results also support the proposal that reopenings occur primarily from the last closed state before opening in the activation sequence since the closed-interval histograms were well described by single exponentials with the mean closed time approximated by $(k_{CO} + k_{CI})^{-1}$.

Aldrich and Stevens (1987) have emphasized that Na channels open only once in N1E115 cells. Careful examination of their shows that near threshold reopening was more common. They estimated the reopening probability to be 0.27, which would cause channel reopenings to account for 40% of the current near threshold. This result is similar to our measurement, although uncertainty as to the membrane potentials in their data as well as in the data from the single-channel patch makes it possible that the near identity of the result is fortuitous. In contrast, Vandenberg and Horn (1984) show that reopening contributed more to the total current than first openings at −40 mV in outside-out patches from their GH_3 cells. This reopening is greater than that seen for either the cardiac channels or the N1E115 channels. Horn and Vandenberg (1986) have offered evidence that the exaggerated reopening behavior seen in their experiments may have resulted from the solutions they used or to changes in kinetics resulting from patch excision. Recently, Kirsch and Brown (1989) offered support for the latter suggestion. They compared Na channel behavior in rat neonatal cardiac ventricular myocytes and rat brain cells in the cell-attached and outside-out configuration. Cardiac Na channels showed more reopening behavior and longer open times than brain channels. Excision further increased reopening and prolonged open times of cardiac channels, but no change was seen in these measures upon patch excision of brain channels. Such a change for the cardiac Na channel could be accounted for by a reduction in k_{OI}. Aldrich and Stevens (1987) also noted that excision of patches from the N1E115 cells altered inactivation characteristics. These observations raise the possibility that the k_{OI} rate constant is under cytoplasmic control in some cells.

Behavior of Na channels in the threshold region is of special importance in heart cells. Under conditions of slow diastolic depolarization during pacemaker events, or during slow or marginal conduction, the initiation of the regenerative upstroke of the action potential depends upon recruitment of Na channel openings in the face of progressive inactivation and offsetting outward currents (Noble and Stein, 1966; Fozzard and Schoenberg, 1972). Detailed knowledge of reopening of Na channels in the threshold region, as well as the rate of inactivation without opening, will be important for understanding the initiation of excitation (e.g., McAllister et al., 1975). These phenomena may be especially important under pathological conditions, when parts of the heart are depolarized by injury.

Voltage-dependent Inactivation

Mean open time initially lengthened with depolarization and then shortened with greater depolarization, showing maximal values between −50 and −40 mV. The biphasic dependence of mean open time in cardiac Na channels has also been reported by Grant and Starmer (1987), Benndorf (1988), and Kirsch and Brown (1989). This behavior is most consistent with processes of opposite voltage dependencies since according to the Markovian model, mean open time is $(k_{OC} + k_{OI})^{-1}$. The shortening with depolarization implies that k_{OI} cannot be constant if k_{OC} is monotonically dependent upon voltage. Maximum likelihood estimation of k_{OI} from single-channel and multichannel patches predicted a modest voltage dependence of 26 mV for an e-fold change (1 e^-). Vandenberg and Horn (1984) found an average voltage dependence of inactivation of 12 mV per e-fold change (2 e^-) for GH_3 cells. Although Aldrich et al. (1983) suggested that inactivation in N1E115 had no voltage dependence, the more detailed analysis of Aldrich and Stevens (1987) showed a modest voltage dependence of 0.3–0.5 e^-. However, k_{OC} only approached k_{OI} in magnitude near threshold; at more positive potentials k_{OI} was much faster than k_{OC}. For both the GH_3 cell and the cardiac cell, on the other hand, k_{OI} is predicted to be much slower and the values cross over k_{OC} at much more depolarized potentials. Whether or not these differences in inactivation voltage dependence between N1E115 cells, GH_3 cells, and cardiac cells represent significant differences in channel properties is not clear. In any case, the calculations provide a basis for experiments that directly examine this behavior.

Inactivation without Opening

Horn et al. (1981) proposed that Na channels can inactivate without opening based on their patch-clamp data. This was demonstrated in depolarizing steps into the voltage range of activation where there were no channel openings. The voltage dependence of this behavior for the single-channel patch is shown in Fig. 9 and for multichannel patches in Fig. 10. P_N was quite high near threshold and one-third to one-half of cycles even near 0 mV failed to elicit openings. The probability of inactivation without opening in terms of the Markovian rate constants is $k_{CF}/(k_{CI} + k_{CO})$. The slope of the Boltzmann fit to the P_N vs. voltage relationship for the multichannel data was about one-half e^- and this can be compared with the prediction of slope by the maximum likelihood calculations (Fig. 14). The voltage dependence of k_{CO} was one e^- and k_{CI} was one-half e^-, and the slope of the P_N Boltzmann was predicted to be 69 mV, or about one-third e^-. One limitation of this analysis is the assumption that k_{CO} and k_{CI} are well described by single exponentials such that the rates continue to increase at more positive potentials. If this is not the case, then P_N need not approach zero but might reach some limiting value. Because at more depolarized potentials channel current is reduced and latency to opening becomes shorter, obscuring some openings in the capacity transient, the presence of a limiting probability is difficult to assess from patch-clamp data.

The slope of the P_N voltage relationship appeared to be steeper for the single-channel patch, and, although there was some inaccuracy involved in assigning voltages because of the bath solution, the data appear to be shifted to more negative potentials compared with the data from the multichannel patches (Fig. 10). This

patch was studied at several degrees warmer temperature than the multichannel patches, and this could mean that the k_{CO} transition rate is more sensitive to temperature than the k_{CI} rate. Some support for this idea has been indirectly suggested by Sheets et al. (1988) in comparing I_{Na} to V_{max} over a range of temperatures and by the observation that time to peak of the macroscopic ionic current has a very high Q_{10}. In support of this as well is the P_N voltage relationship published by Benndorf (1988) at room temperature. In this case P_N was a quite steep function of voltage, and the relationship was displaced in the negative direction.

Methodological Limitations

The single-channel data were obtained over a limited voltage range, because of the need to maintain a signal-to-noise ratio of over six. On the other hand, the voltage range included both the threshold and the plateau regions of the cardiac Purkinje cell action potential. The experimental protocols were also limited to step depolarizations, while more complex protocols would have aided in sorting out some aspects of the Markovian model.

The five-state model, as well as the simpler models considered, reproduced observed open-duration data and reopening behavior, but resulted in $P_{open}(t)$ that consistently underestimated P_{open} at peak and produced only a single exponential decline in current. Consequently, the more complex behavior of current decay found in heart cells requires some change in the model. Chiu (1977) suggested a model with an intermediate state on the path to the absorbing inactivated one, and such a change would be expected to produce two time constants for current decay, one faster and one slower than that produced by the five-state model used here. This modification would also be expected to speed the estimate of the rate of activation and to improve the estimate of P_{open} at peak. Some evidence exists that the Na channel may have more than one open state (Kunze et al., 1985; Nagy, 1987). The present analysis assumed only one open state, consistent with our own data. We could not exclude the possibility that there was another open state with a similar value of conductance and similar kinetics.

The most important assumption in our data analysis is that the kinetic behavior of the Na channel can be represented by a Markovian model with a small number of states. The advantage of such an analysis is that it organizes channel behavior into smaller, more manageable steps with convenient descriptors that may correlate with molecular events. For a more detailed discussion of this approach, see French and Horn (1983) and Horn and Vandenberg (1984). Our only data inputs used to evaluate this model were the times of opening and closing of channels upon step depolarizations, so that estimates of transition rates for states distant from the open state were progressively more unreliable and slow back reaction rates could not be estimated. The use of larger numbers of states would increase the number of adjustable parameters and improve fits to discrete data, but would be unlikely to maintain adequate levels of accuracy. Integration of other methods of Na channel characterization, such as gating current, will be of value in interpreting channel behavior prior to channel opening.

In summary, we have used single-channel recordings from isolated canine cardiac Purkinje cells to characterize activation and inactivation behavior of Na channels.

Channel reopening and inactivation without opening were prominent near threshold, and mean open times showed a biphasic voltage dependency. The single-channel data were analyzed by the histogram and the maximum likelihood methods, using a simple Markov model of channel states. The results showed that behavior of the cardiac Na channel was dominated by its activation kinetics, but that inactivation was also voltage dependent. The behavior of the cardiac Na channel is much like that of the GH_3 pituitary cell and the N1E115 neuroblastoma cell, with only small changes in the values of some of the channel transition rate necessary to account for the behavior of all three channel types.

Note added in proof. Some of these results are similar to those recently reported by Yue et al. (1989. *Science.* 244:349–352) and Berman et al. (1989. *Journal of Physiology.* 415:503–531).

This work was supported by US Public Health Services grants 5T32GM0728 (B. E. Scanley) and 5PO1HL20592. T. R. Chay was supported by grants from the US Public Health Services (R01-HL33905) and the National Science Foundation (82-15582).

Original version received 14 June 1988 and accepted version received 21 August 1989.

REFERENCES

Aldrich, R. W., D. P. Corey, and C. F. Stevens. 1983. A reinterpretation of mammalian sodium channel gating based on single channel recording. *Nature.* 306:436–441.

Aldrich, R. W., and C. F. Stevens. 1987. Voltage-dependent gating of single sodium channels from mammalian neuroblastoma cells. *Journal of Neuroscience.* 7:418–431.

Benndorf, K. 1988. Patch clamp analysis of Na channel gating in mammalian myocardium. *General Physiology and Biophysics.* 7:353–378.

Benoit, E., A. Corbier, and J. M. DuBois. 1985. Evidence for two transient sodium currents in the frog node of Ranvier. *Journal of Physiology.* 361:339–360.

Brown, A. M., K. S. Lee, and T. Powell. 1981. Sodium currents in single rat heart muscle cells. *Journal of Physiology.* 318:479–500.

Cachelin, A. B., J. E. DePeyer, S. Kokubun, and H. Reuter. 1983. Sodium channels in cultured cardiac cells. *Journal of Physiology.* 340:389–401.

Chay, T. R. 1988. Kinetic modeling for the channel gating processes from single channel patch clamp studies. *Journal of Theoretical Biology.* 132:449–468.

Chiu, S. Y. 1977. Inactivation of sodium channels second order kinetics in myelinated nerve. *Journal of Physiology.* 273:573–596.

Colquhoun, D., and A. G. Hawkes. 1977. Relaxation and fluctuations of membrane current that flow through drug-operated channels. *Proceedings of the Royal Society of London.* 199:231–261.

Colquhoun, D., and F. J. Sigworth. 1983. Fitting and statistical analysis of single-channel records. *In* Single Channel Recording. B. Sakmann and E. Neher, editors. Plenum Publishing Co., New York. 191–263.

Fernandez, J. M., A. P. Fox, and S. Krasne. 1984. Membrane patches and whole cell membranes: a comparison of electrical properties in rat clonal pituitary (GH_3) cells. *Journal of Physiology.* 356:565–585.

Fozzard, H. A., D. A. Hanck, J. C. Makielski, B. E. Scanley, and M. F. Sheets. 1987. Sodium channels in cardiac Purkinje cells. *Experientia.* 43:1162–1168.

Fozzard, H. A., and M. Schoenberg. 1972. Strength-duration curves in cardiac Purkinje fibres: effects of liminal length and charge redistribution. *Journal of Physiology.* 225:593–618.

French, R. J., and R. Horn. 1983. Sodium channel gating: models, mimics and modifiers. *Annual Review of Biophysics and Bioengineering.* 12:319–356.

Grant, A. O., and C. F. Starmer. 1987. Mechanisms of closure of cardiac sodium channels in rabbit ventricular myocytes: single channel analysis. *Circulation Research.* 60:897–913.

Grant, A. O., C. F. Starmer, and H. C. Strauss. 1983. Unitary sodium channels in isolated cardiac myocytes of rabbit. *Circulation Research.* 53:823–829.

Hanck, D. A., M. F. Sheets, and H. A. Fozzard. 1990. Gating currents associated with Na channels in canine cardiac Purkinje cells. *Journal of General Physiology.* 95:439–457.

Horn, R., and K. Lange. 1983. Estimating kinetic constants from single channel data. *Biophysical Journal.* 43:207–223.

Horn, R., J. Patlak, and C. Stevens. 1981. Sodium channels need not open before they inactivate. *Nature.* 291:426–427.

Horn, R., and C. A. Vandenberg. 1984. Statistical properties of single sodium channels. *Journal of General Physiology.* 84:505–534.

Horn, R., and C. A. Vandenberg. 1986. Inactivation of single sodium channels. *In* Ion Channels in Neural Membranes. Journal Ritchie and R. Keynes, editors. Alan R. Liss, New York. 71–83.

Kirsch, G. E., and A. M. Brown. 1989. Kinetic properties of sodium channels in rat heart and rat brain. *Journal of General Physiology.* 93:85–99.

Kiyosue, T., and M. Arita. 1989. The late sodium current and its contribution to action potential configuration in guinea pig ventricular myocytes. *Circulation Research.* 64:389–397.

Kohlhardt, M., V. Frobe, and J. W. Herzig. 1986. Modification of single cardiac Na^+ channels by DPI 201-106. *Journal of Membrane Biology.* 89:163–172.

Kunze, D. L., A. E. Lacerda, D. L. Wilson, and A. M. Brown. 1985. Cardiac Na currents and the inactivity, reopening, and waiting properties of single cardiac Na channels. *Journal of General Physiology.* 86:697–719.

McAllister, R. E., D. Noble, and R. W. Tsien. 1975. Reconstruction of the electrical activity of cardiac Purkinje fibres. *Journal of Physiology.* 251:1–59.

Makielski, J. C., M. F. Sheets, D. A. Hanck, C. T. January, and H. A. Fozzard. 1987. Sodium current in voltage clamped internally perfused canine cardiac Purkinje cells. *Biophysical Journal.* 52:1–11.

Nagy, K. 1987. Evidence for multiple open states of sodium channels in neuroblastoma cells. *Journal of Membrane Biology.* 96:251–262.

Noble, D., and R. B. Stein. 1966. The threshold conditions for initiation of action potentials by excitable cells. *Journal of Physiology.* 187:129–162.

Noda, M., T. Ikeda, T. Kayano, H. Suzuki, H. Takeshima, M. Kurasaki, H. Takahashi, and S. Numa. 1986. Existence of distinct sodium channel messenger RNA's in rat brain. *Nature.* 320:188–192.

Patlak, J. B., and R. Horn. 1982. Effect of *N*-bromoacetamide on single sodium channel currents in excised membrane patches. *Journal of General Physiology.* 79:333–352.

Patlak, J. B., and M. Ortiz. 1985. Slow currents through sodium channels of the adult rat heart. *Journal of General Physiology.* 86:89–104.

Rogart, R. B., L. L. Cribbs, L. K. Muglia, M. W. Kaiser, and D. D. Kephart. 1989. Molecular cloning of a putative tetrodotoxin-resistant rat heart Na^+ channel isoform. *Proceedings of the National Academy of Sciences.* 86:8170–8174.

Scanley, B. E., D. A. Hanck, M. F. Sheets, and H. A. Fozzard. 1985. Reopening behavior of Na channels in isolated canine cardiac Purkinje cells. *Journal of General Physiology.* 86:12*a*. (Abstr.)

Scanley, B. E., and H. A. Fozzard. 1987. Low conductance sodium channels in canine cardiac Purkinje cells. *Biophysical Journal.* 52:489–495.

Sheets, M. F., D. A. Hanck, and H. A. Fozzard. 1988. Nonlinear relation between V_{max} and K_{Na} in canine cardiac Purkinje cells. *Circulation Research.* 63:386–398.

Sheets, M. F., January, C. T. and H. A. Fozzard. 1983. Isolation and characterization of single canine Purkinje cells. *Circulation Research.* 53:544–548.

Sigworth, F. J., and E. Neher. 1980. Single Na channel currents observed in cultured rat muscle cells. *Nature.* 287:447–449.

Sills, M. N., Y. C. Xu, E. Baracchini, R. H. Goodman, S. S. Cooperman, G. Mandel, and K. R. Chien. 1989. Expression of diverse Na^+ channel messenger RNA's in rat myocardium. *Journal of Clinical Investigation.* 84:331–336.

Vandenberg, C. A., and R. Horn. 1984. Inactivation viewed through single sodium channels. *Journal of General Physiology.* 84:535–564.